



Utilizing image processing in prediction of kidney function

M. S. El Nagdy^{a*}, Safaa L. Diab^a, H. M. Yassin^b

^a Physics Department, Faculty of Science, Helwan University

^b King Fahd Unit, Faculty of Medicine, Cairo University

ARTICLE INFO

Article history:

Received 24 February 2023

Accepted 8 March 2023

Available online 4 June 2023

doi: [10.21608/ABAS.2023.195716.1012](https://doi.org/10.21608/ABAS.2023.195716.1012)

Keywords: kidney glomerular filtration rate, kidney function

ABSTRACT

Renal scintigraphy has been used widely to measure the individual kidney glomerular filtration rate (IKGFR). Glomerular filtration rate (GFR) is a key parameter in evaluating kidney function. After a bolus injection of an exogenous GFR marker in plasma an accurate determination of GFR can be made by measuring the marker concentration in plasma during the excretion. In this research a new algorithm is developed and tested two new parameters to diagnose the status of human kidneys function. The two parameters give good prediction to the kidney status that complies with the GFR. The two parameters are better, where they diagnose the kidney in the real time at very low cost.

1. Introduction

Image processing in medicine may play a significant role to help the doctors in investigating the interior portions of the body for easy diagnosis. Artificial intelligence methods such as neural network [1-3] were used as a way to perform pattern recognition tasks. Renal expert system (RENEX) has been developed to assist physicians to detect renal obstruction. A renal expert system was developed by Carcia EV, et al [4] who extracted 47 quantitative parameters from 99mTC-MAG3 scans of 100 potential renal donors. Processing time per patient was practically instantons. Andrew Tayler, et al [5] compared diuresis renography scan generated by renal expert system with the consensus interpretation of expert readers. High level of agreement between RENEX and consensus results indicates that RENEX is performing similarly to each of the expert readers. Statistical approach called log-linear

modeling was presented by Amita, et al [6] who found that this approach can fully characterize the accuracy of computer-aided diagnosis tool. The effect of an angiotensin-converting enzyme inhibitor (enalapril) on renal function was evaluated by Shady, et al [7]. El-Nagdy, et al [8] compared the renogram curves of 99m-MDP to that of 99mTC-DTPA based on the curve pattern and time to peak activity. From previous research it is notice that renogram images of non-obstructed kidney are smoothness in gray level but it does not smooth in case of obstructed cases. In fact, implementations of decision support tools have the potential to help physicians interpret low volume studies at a faster rate and with higher level of confidence. In this context the authors develop an algorithm to help physicians to give instantons decision with high level of confidence.

2. Experimental work

* Corresponding author E-mail: physicshelwan@yahoo.com

2.1 Materials and Methods

The patients were referred for evaluation of renal function and pathophysiology in routine practice. They were given a wide variety of clinical diagnosis including chronic renal failure, hydronephrosis, reduced renal function in an unknown cause and healthy persons for donation.

2.2 Venography

^{99m}Tc -DTPA was prepared in Radioisotope Laboratories in King Fahd Unit, Cairo University Hospitals (Egypt) using a commercially available freeze-dried kit. The dose was ranged from 3.5 to 6.5 mCi and was administered to number of patients with different renal disease and healthy persons. Prior to the administration, the pre-injection syringe with straight needle was counted by two different devices: 1) Dose Calibrator (ATOMLAB 100) and 2) Gamma Camera (Siemen, Orbit, Single head), which was attached to a Low-Energy General-Purpose Parallel-Hole Collimator as shown in Figure. The patient was hydrated with 300-500 ml of water 30 minutes prior to the examination. The patient lay down on a bed in the supine position and the image will acquired a posterior except one patient with ectopic kidney lay down on a bed in the prone position. ^{99m}Tc -DTPA was given through a butterfly needle into vein and was followed by infusion of 20 ml of normal saline then 2 ml lasix. Frames of 128×128 matrix were recorded with an online-computer, initially at one second for one minute and then at 10 seconds for 20 minutes. The post-injection syringe with a straight needle which was detached before the injection was again counted by a gamma camera in the same way as pre-injection. Region of interest (ROI) over each kidney was assigned manually on the frame added from 1 to 3 minutes following injection. The semilunar background ROI around each kidney was defined. The background corrected time-activity curve was generated, and the renal uptake of individual kidney for one minute from 2 to 3 minutes after the injection was calculated. The GFR (GFR Gates) was automatically estimated by a commercially available computer (Oddesey Pegasus Laboratories, Adac) according to the Gates' algorithm.

2.3 Standard protocol for calculation of GFR

Peak time (second). The peak time is the time interval from the start of the acquisition to the time that the curve reaches the maximum count. Half peak time (second) The Half Peak Time ($\frac{1}{2}$ peak time) is the time interval from the peak time to the time that the curve reaches half the maximum counts. For example, if the peak occurs at 400 seconds and the half peak occurs at 1600 second, then the half peak time is 1200 seconds. Note: A zero value indicates that the application did not find a half peak. Depth (cm). It is the calculated depth from the body surface to the kidney's center. Uptake (%) It is the background-corrected, kidney count uptake from two to three minutes after the acquisition was started. GFR (ml/min). It is the glomerular filtration rate measured in ml/min. Total GFR (ml/min). The total GFR is the sum of the

GFR for both the right and left kidneys. Normalized GFR (ml/min). The normalized GFR is normalized to the body surface area by dividing 1.73 m² by the body surface area. Calculated based on height and weight, and then multiplying the result by the GFR. The percent renal uptake in the GFR equation is calculated according to equation. The percent uptake of the left kidney plus the percent uptake of the right kidney, at 2 to 3 minutes post-injection is calculated by dividing the background and depth-corrected kidney counts by the total net counts injected and multiplying the result by 100. In this equation, μ is the attenuation coefficient of ^{99m}Tc in soft tissues equals 0.153, and x is the kidney depth in centimeters. These values (the normalized and depth-corrected kidney counts and the total net counts) are obtained from the nuclear medicine renogram study. The total net counts injected are determined by the pre-injection syringe and post-injection syringe images. The post-injection counts are then corrected for decay to compensate for "excess time" between the pre-injection image and post-injection image. Finally, the decay-corrected, post-injection syringe counts are subtracted from the pre-injection syringe counts to yield the total net counts injected. The normalized and corrected kidney counts are determined from 60 seconds of data collected 2 to 3 minutes following tracer arrival in the kidney. To permit accurate sampling of the renal uptake, a dynamic study in a 128×128 matrix is acquired at 10 to 15 seconds/frame for 6 minutes, immediately following tracer administration. A composite image is created from the dynamic study. Areas of interest are created for each kidney and for the corresponding background areas. The background areas are then normalized to their respective renal areas and the counts in the normalized background areas are subtracted from the counts in the renal areas to give the normalized net kidney counts.

The following data are required to run the GFR application:

- Pre-injection and post-injection count calibration images of the syringe containing the radiopharmaceutical. These are 60-seconds static images with matrix size up to 512×512 and 8-bit or 16-bit deep acquired 30 cm from the detector face (including padding).
- A dynamic image or a variable framing rate (VFR) dynamic image acquired for a minimum of 6 minutes.
- matrix size up to 128×128 , 16-bit deep, n seconds-per-frame, n frames, and labeled renal flow
- using a VFR image with a flow component, the image's first phase is assumed to be the flow. The flow phase can be any matrix size up to 128×128 , 16-bit deep, n seconds-per-frame, n frames, and duration of n seconds and labeled flow.
- The image's second phase can be any matrix size up to 128×128 , 16-bit deep, n seconds-per-frame, n frames, and labeled function. If using a VFR image without a flow component.

3. The developed algorithm

The purpose of this algorithm is to develop a new coefficient to classify each kidney as an obstructed or non-obstructed. The steps of the algorithm are exhibited in Fig. (1) and summarize as follows:

1. Renogram image is captured and is processed by using the Matlab. software [9] that is used to specify each kidney with its gray levels.
2. Let z denote a discrete random variable representing discrete gray levels in the rang $[0, L-1]$; $L=256$, the lowest value of L corresponding the dark pixels of the image and high value of L corresponding the bright pixels of the image.

Let $p(z_i)$ be the corresponding histogram,

$i = 0,1,2,3, \dots, L - 1$ $p(z)$ estimate of the probability of occurrence of gray level z_i Type equation here.

3. The histogram is computed for each kidney, the relative bright area (RBA) of the kidney can be computed and the variance $\sigma(z)^2$ of the gray levels can be computed also. A parameter of relative smoothness (RS) of the gray level can be computed using the equation given below [10,11]:

$$R = 1 - \frac{1}{1 + \sigma(z)^2}$$

R approaches zero for area of constant intensity (the variance is zero) and approaches 1 for large values of $\sigma(z)^2$. The variance is normalized to the interval $[0,1]$ [10,11]. This is done simply by dividing $\sigma(z)^2$ by $(L - 1)^2$, L is the number of distinct gray levels.

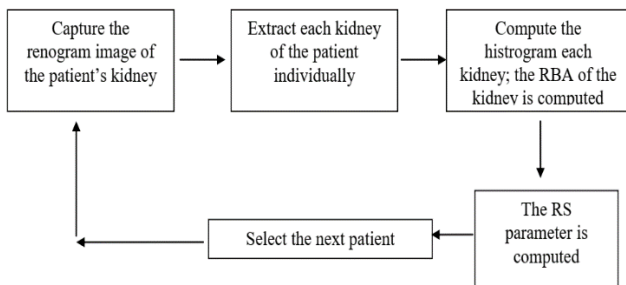
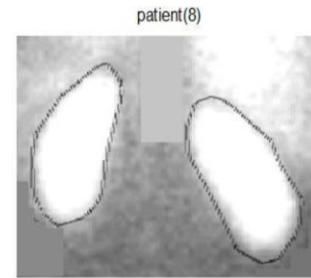


Fig.1: Flow chart of developed algorithm.

2. Results and discussion

The developed algorithm is applied to compute RS and RBA for each kidney of 23 patients. Figure (2) represents the renogram image of a patient of non-obstructed case. Edges of left and right are defined and shown in Figure (3) and Figure (5) respectively. Reconstruction of each kidney with different gray levels are represented in figures (4,6), respectively.

The RS and RBA of 23 patients are computed for each kidney, the results are tabulated to show the correspondence of the RS and the GFR as illustrated in table (1) for non-obstructed cases. The correspondence of the RS and the GFR for obstructed cases are illustrated in table (2). The data of the lift kidney in Table 1 and Table 2 is graphed in figure (7), to compare the values of RS in both cases of the obstructed case and non- obstructed cases.



Figure(2)

Edges of left kidney



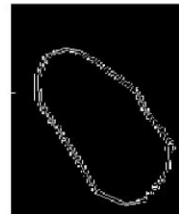
Figure(3)

The reconstructed left kidney



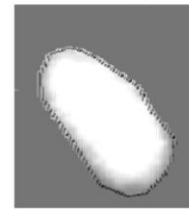
Figure(4)

The edges of right kidney



Figure(5)

The reconstructed right kidney



Figure(6)

It is clear that the values of the RS are higher in the non-obstructed cases than those of the obstructed cases. Accordingly, when the RS value exceeds 0.0022, one can conclude with high probability that the kidney is non-obstructed. However, when the case is boarder (the GFR value is close to 80 or 120), the value of smoothness may be misleading. And this feature is also characterized in the GFR. To overcome and enhance the performance of the RS in predict the kidney status, another parameter was developed which is called 'RBA'. The data of the lift-kidney in table 1 and table 2 is graphed in figure (8), of RBA in both cases of the obstructed case and non- obstructed cases, to compare the values of the RBA in both cases of the obstructed cases and non- obstructed cases. It is obvious that there is a clear difference between the values of RBA in cases of non-obstructed and obstructed kidney. One can claim that if the

value of RBA parameter is 0.45 or more, the kidney is most probably non-obstructed. However, the problem of the border cases ($GFR \cong 120$) the results of the parameter may be misleading. When the value of GFR go larger (a clear obstructed cases) the RBA will give good prediction. The results of the right kidneys in Tables (1 and 2) support the inferential concluded from the left kidneys results. The maximum values and minimum values for the two kidneys differ by no more than 0.05%.

Table 1: Non Obstructed Case

Patient no.	GFR	RS of left kidney	RS of right kidney	The RBA of Left Kidney	The RB A of Right Kidney
1	97.44	0.0024	0.0359	0.5333	0.527
2	106.01	0.0027	0.0025	0.6753	0.5757
3	85.86	0.0027	0.0024	0.556	0.5172
4	91	0.0023	0.0024	0.6534	0.5172
5	95.24	0.0023	0.0019	0.463	0.0932
6	117.54	0.0023	0.0023	0.207	0.575
7	106.15	0.0024	0.0025	0.495	0.618
8	111.17	0.0025	0.0026	0.592	0.616
9	103.53	0.0028	0.0026	0.701	0.4815
10	118.91	0.0026	0.0023	0.6151	0.5534
11	91.43	0.0027	0.0024	0.655	0.5701
12	104.9	0.0027	0.0026	0.6242	0.487
13	96.47	0.0028	0.0025	0.675	
				0.6642	
Max	118.91	0.0028	0.0359	0.701	
					0.0932
Min	85.86	0.0023	0.0015	0.207	

Table 2: Obstructed Case

Patient no.	GFR	RS of left kidney	RS of right kidney	The RBA of Left Kidney	The RBA ³ of Right Kidney
1	71.65	0.0015	0.0015	0.09	0.103
2	34.29	0.0014	0.0015	0.108	0.0834
3	126.57	0.0026	0.0025	0.628	0.568
4	77.15	0.0012	0.0014	0.185	0.1211
5	130.92	0.0022	0.0025	0.397	0.577
6	138.45	0.0023	0.0023	0.464	0.4774
7	123.68	0.0015	0.0016	0.087	0.073
8	73.91	0.0014	0.0015	0.12	0.1
9	75.78	0.0017	0.0014	0.09	0.2
10	128	0.0014	0.0015	0.0959	0.0932
Max	138.45	0.0026	0.0025	0.628	0.577
Min	34.29	0.0012	0.0014	0.087	0.073

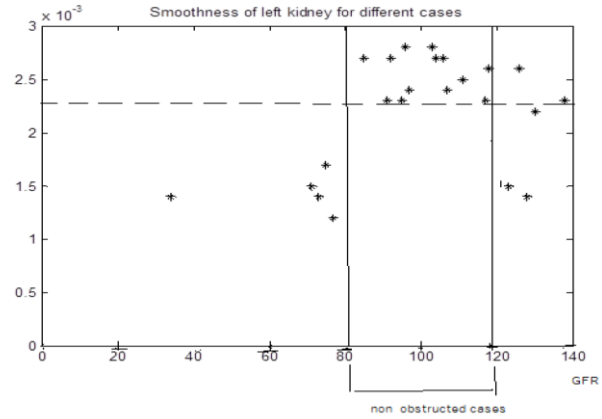


Fig. 7: The correspondence of the RS and the GFR for 23 cases

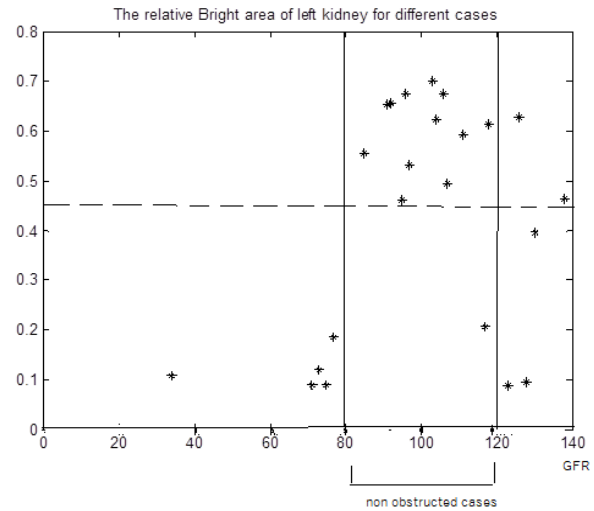


Fig. 8: The correspondence of the RBA and the GFR for 23 cases.

Conclusions

In this research, the image processing techniques were employed to diagnose the status of human kidneys whether it is obstructed or non-obstructed. A medical factor, namely GFR, is used as a reference where it indicates that the kidney is non-obstructed when $80 < GFR < 120$ kidney is non-obstructed and is obstructed otherwise. Two different parameters were developed to test the kidney status; RS and RBA. The two parameters RS and RBA give good prediction of the kidney status that comply with the GFR. The big advantage of these parameters is that they can give the status of each kidney alone while the GFR show if the two kidneys are obstructed or non-obstructed; and a further investigation is needed to know which kidney is specifically obstructed. In addition, the parameters are better, where they diagnose the kidney status in the real time at very low cost.

References

1. Hiroshi Fujita, tetsuro Katafuchi, Toshiisa Uehara, and Tsunehiko Nishimura, "Application of Artificial Neural Network to Computer-Aided Diagnosis of coronary Artery Disease in Myocardial SPECT Bull's-eye Images", *Journal of Nuclear Medicine*, 1992, 33: 272
2. Gerold Porenta, Georg Dorffner, Stephan Kundrat, Paolo Petta, Johanna Duit-Schedlmayer and Heinz Sochor, "Automated Interpretation of Planar Thallium-201-Dipyridamole Stress-Redistribution scintigrams Using Artificial neural Networks", *Journal of nuclear medicine*, 1994, 35: 2041.
3. Hamilton D, Riley PJ, Miola UJ, Amro A A, "A feed forward Neural Network for classification of bull's-eye myocardial Perfusion images", *Journal of nuclear medicine*, 1995, 22(2), 108.
4. Grcia EV, Taylor A, Halkar R, Folks R, Krishnan M, Cooke CD, Dubovsky E., "An expert system for the interpretation of ^{99m}Tc -MAG3 Scans to detect renal obstruction", *Journal of nuclear medicine*, 2006, 47(2): 320.
5. Andrew Taylor, Ernest V. Garcia, Jose Nilo G. Binongo, Amita Manatunga, Raghuv eer halkar, Russell D. Folks, and Eva dubovsky, "Diagnostic Performance of an Expert system for Interpretation of ^{99m}Tc MAG3 scans in Suspected Renal obstruction", *Journal of nuclear medicine*, 2008, 49: 216.
6. Amita K Manatunga, Jose Nilo G Binongo and Andrew T Taylor "Computer-aided diagnosis of renal obstruction: utility of log-Linear modeling vsus Standard ROC and Kappa analysis", *EJNMMI Research*, 2011, 1: 1
7. Shady A. Soliman, Ahmed A. Shokeir, Ahmed Mosbah, Hassan Abol-Enein, Nashwa Barakat, Essam Abou-Bieh, Ehab W. Wafa, "Recoverability of Renal function After Relief of Chronic Partial Ureteral Obstruction: Study of the Effect of Angiotensin Receptor Blocker (Losartan)", 2011, 75:848.
8. Amer H. H., NAGDY. M.S. and YASSIN H.M., "Quantitative Assessment of Renal Function with ^{99m}Tc -MDP in Comparison with ^{99m}Tc -DTPA", *Isotope & Rad. Res.*, 2011, 43(1): 285.
9. Thompsom clay M, Shure Loren "Image Processing Toolbox. Natick the Math works Inc." 2004.
10. Jain Anil K. Wood Richard E. "Digital Image Procwssing. New Jersey; Prentic-Hall, Inc." 2002.
11. Gonalez Rafaelc, woods Richard E. "Digital Image Processing. New Jersey; Prentic-Hall, Inc" 2002.